The search for γ-ray emission from AE Aquarii using Fermi-LAT Pass 8 Data pipeline 2008-2018

ST Madzime, HJ van Heerden, PJ Meintjes, A Odendaal, RJ Britto
Department of Physics, University of the Free State, Bloemfontein, South Africa

E-mail: madizimest@ufs.ac.za, VanHeerden@ufs.ac.za, MeintjPJ@ufs.ac.za, winka@ufs.ac.za

Abstract. We present the preliminary results of the search for gamma-ray emission from AE Aquarii (AE Aqr) using the upgraded Ferm-LAT Pass 8 data analysis pipeline. A previous study using the Fermi-LAT Pass 7 data pipeline showed low-level but consistent, pulsed emission at a period of 16.54 seconds, which is the first harmonic of the 33.08 s pulsed emission at the spin period of the white dwarf. This implies possible gamma-ray emission from both polar caps of the spinning white dwarf. A re-analysis with the Pass 8 data pipeline, which uses an improved galactic diffuse gamma-ray emission model as well as more inclusive selection criteria, has resulted in no detection of any gamma-ray emission from AE Aqr according to the Fermi-LAT detection threshold. However, three spectral points with significance just above 2σ were detected according to *fermipy*'s spectral points detection threshold.

1. Introduction

AE Aqr is a cataclysmic variable close binary which consists of a fast rotating magnetized white dwarf orbiting a late-type main sequence companion (K4-5) star, with an orbital period of 9.88 hrs (e.g [1, 2, 3]). The white dwarf is highly magnetic ($\sim 10^6$ Gauss) and rotates with a period of $\sim$ 33 s [4]. AE Aqr exhibits nova-like characteristics in the optical waveband with a visual magnitude varying between $m_v = 10$ and $m_v = 12$ [5].

Initially, the system was erroneously classified as a DQ Her system, based on some similarities with DQ Hercules. However, later studies revealed that the system is significantly different since the white dwarf currently accretes very little material as a result of the magnetospheric propellering of materials from the fast rotating white dwarf magnetosphere, which drives the mass-flow from the secondary star out of the binary system [6, 7].

Non-thermal radio emission from AE Aqr was first detected by Bookbinder & Lamb (1987) [8]. This emission was later shown to be highly transient, showing flaring activity with flux levels varying between 1 and 12 mJy [9] on a continuous basis. In contrast to the initial perception that radio and optical outbursts could be associated with enhancements in the accretion rate onto the white dwarf, Patterson (1979) [10] showed that there was no significant increase in the pulsed fraction of the periodic optical emission during flares. It was shown [11] that a fragmented blobby mass transfer stream from the secondary star ejected by the fast rotating white dwarf (i.e. a magnetospheric propeller) could, in fact, drive the optical flaring, which explains why the pulsed fraction of the 33.08 s rotation period does not increase significantly during the flaring. It has been shown [12] that the white dwarf in AE Aqr could readily accelerate electrons and protons to energies of the order of several TeV (1 TeV = 10^{12} eV), which could provide gamma

rays through leptonic channels (synchrotron, inverse Compton) or a hadronic channel (neutral pion production and decay to gamma rays). These accelerated electrons, continuously pumped by the sweeping white dwarf magnetosphere, also produce non-thermal radio to infrared (IR) flaring emission with the observed van der Laan - type Spectral Energy Distribution (SED) [13].

The transient non-thermal radio flares observed from AE Aquarii, and its similarities with Cyg X-3 (albeit at a lower level), provided the first motivation to embark on a search for TeV emission from this source (see e.g. [14, 15, 16, 17]). Recently a Fermi-LAT search by van Heerden [18], using the Pass 7 pipeline, revealed weak but consistent pulsations at the first harmonic ($\sim$ 16.54 s) of the 33.08 s spin period of the white dwarf. In this paper, the preliminary analysis and results in the search for gamma-ray emission from AE Aquarii utilizing Fermi-Pass 8 data will be presented.

2. Data Reduction & Analysis

The archival gamma-ray data from Fermi Large Area Telescope (Fermi-LAT) observed between 4 Aug 2008 to 2 May 2018 were considered. The data comprises of all Fermi-LAT events and spacecraft data. The analysis of the Fermi LAT data were performed using python software *fermipy* (v 0.17.3), which is part of the Fermi Science Tools software packages (v11r0p5). We used the (iso_P8R2_SOURCE_V6_v06.txt) set of response functions and selected corresponding source−class events, events class (evclass=128) and front+back events type (evtype=3). In this analysis, photons were selected from a radius of 10 degrees Region Of Interest (ROI), centered at the optical coordinates of AE Aquarii (RA=310.038, DEC= -0.8708). The zenith angle cut was set at 90 degrees to avoid contamination by photons produced from cosmic-ray interactions with the atmosphere. Binned maximum -log(likelihood) analysis was performed on the energy range 0.1-500 GeV. All sources within 20 degrees of ROI, the instrumental background (iso_P8R2_SOURCE_V6_v06.txt), and the diffuse galactic emission model (gll_iem_v06.fits, [19] as well as the source of interest were used to generate the spectral-spatial model using the python module (make3FGLxml.py). The analysis of AE Aqr was performed utilizing the simplest spectral model for non-thermal emission (i.e a Power Law see equation (1)).

$$\frac{dN}{dE} = N_o \left[\frac{-E}{E_o}\right]^{-\Gamma} \tag{1}$$

The power law model requires three parameters: the power law index (Γ) which controls the hardness of the source, the scale (N_o), this is the normalization factor to scale the observed brightness of the source and the prefactor (E_o), which scales the energy. These parameters and other parameters in the spectral-spatial model were optimized and fitted using the maximum -log(likelihood) technique, [20]. The significance of AE Aqr was assessed using the ratio of -log(likelihood) L. This ratio is known as the test statistics (TS) as shown by equation 2,

$$TS = -2log\left(\frac{L_{max,0}}{L_{max,1}}\right) \tag{2}$$

where $L_{max,0}$ is the maximum likelihood value for a model without an additional source (the null hypothesis) and $L_{max,1}$ is the maximum likelihood value for a model with the additional source at a specified location. The term significance in this analysis is defined in σ units, where it is assumed to take the square-root value of TS [20]. Fermi-LAT sources with test statistic less than 25 were removed from the fit, and to get the desired fit status and quality for the model, the parameters of all sources beyond a 5 degrees angular distance from the centre of the ROI were fixed, whereas those of the target source were set free.

Fermipy has several processes and analysis output product that can be used to search for un-modelled sources as well as evaluating the fit quality of the model. These include TS-Map,

TS-Cube, Residual-Map and Source Finding. In this analysis, TS and Residual maps were employed and the Spectral Energy Distribution (SED) was computed.

3. Results

The average TS for AE Aquarii from *fermipy* binned analysis was zero in the energy range 0.1-500 GeV. This value is way below the detection limit which means that the proposed spectral model does not characterize the source correctly, or that the target is not a strong enough emitter to be classified as a gamma-ray source. The left-hand side of Figure 1, shows a counts map of filtered raw data with Good Time Intervals (GTIs') applied and the right-hand side the likelihood model map, which shows all sources that were included in the fit.

.

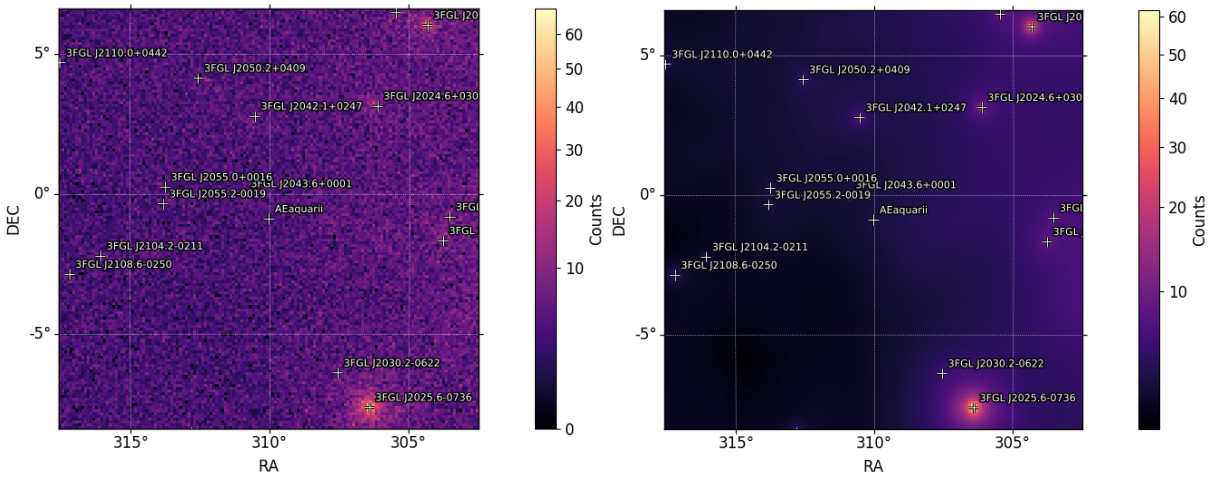

Figure 1: Counts map (left) and model map (right). The counts map is the cumulative data of observed counts at a given grid location. A closer inspection of the counts map generated for ten years of data shows that there are no extremely bright sources in the ROI.

3.1. TS and Residual Maps

TS maps were generated for the entire ROI, using the *gta.tsmaps()* routine which generates a TS map for each source component in the model centered at each spatial bin. TS maps are only sensitive to a positive deviation with respect to the model. The method calculates TS for each bin using equation (2). The TS map on the left-hand side of Figure 2 shows no gamma-ray significance, this corresponds well with the analysis results. On the right-hand side is the residual map generated by the *gta.residmap()* routine, which calculates the residual between the counts' map and model map. The residual map is sensitive to positive and negative deviations. There should be no region with an excess in terms of significance if the model describes the data well.

3.2. Spectral energy distribution (SED)

Additional to TS maps, SED points with 30 energy bins per decade and butterfly plots were generated to see whether the model is in agreement with the data and also to check which energy bins contribute more to the obtained TS. On the left-hand side of Figure 3 is a SED plot fitted with a power law, butterfly plots are also included on the fit and on the right-hand side a broadband SED, with plotted points from this study, archival data, and CTA, and Fermi-LAT sensitivity curves. Further investigations on the energy bins with significance just above 2σ is presented in Fig 4, with energy range between 0.4 and 10 GeV.

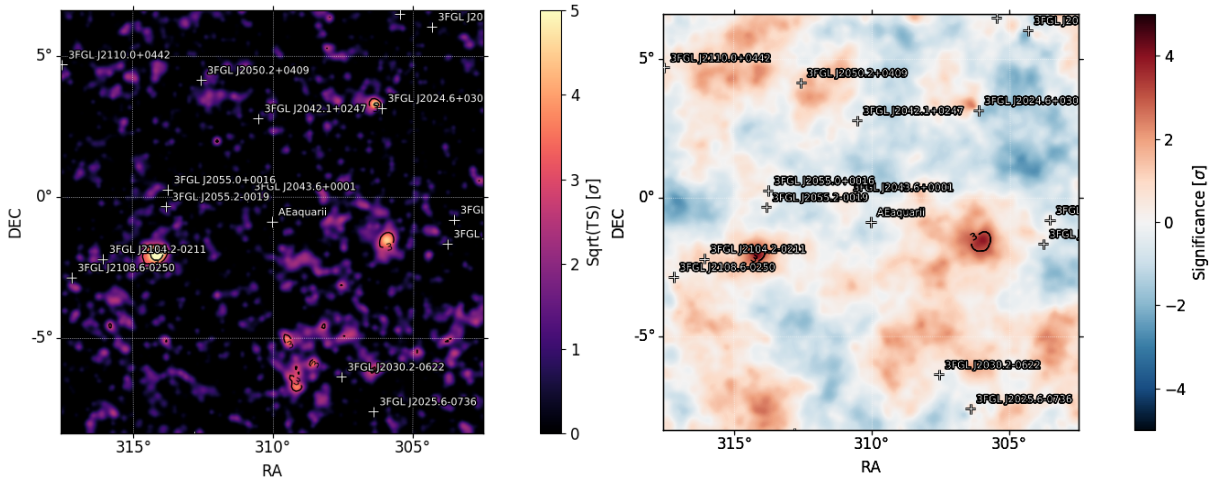

Figure 2: The TS map on the left shows the significance of all sources included in the model, and a residual map is provided on the right.

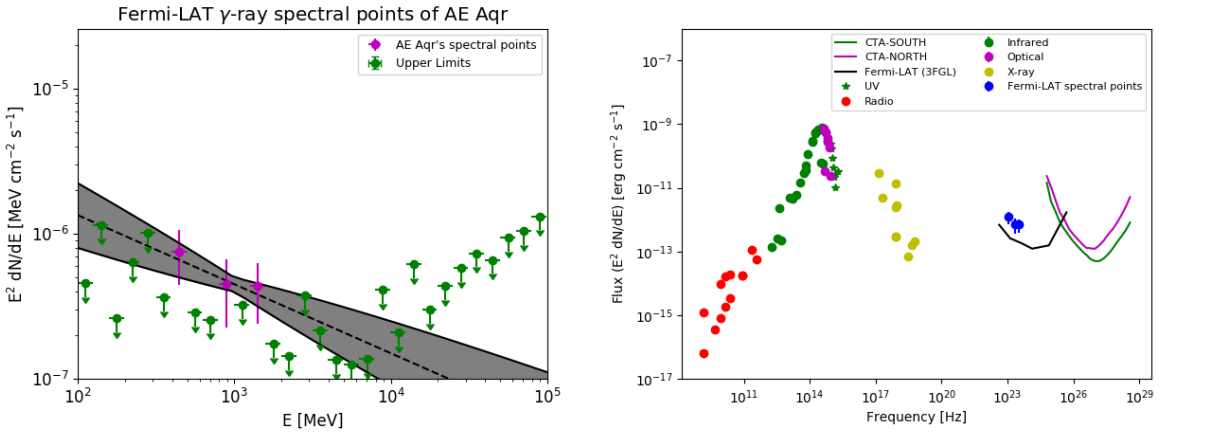

Figure 3: Fermi-LAT spectral points, upper limits, and butterfly plot of AE Aqr (left), and the spectral broad band of AE Aqr from radio to higher energy (right).

4. Discussion & Conclusion

This study resulted in no detection of gamma-ray emission from the region of AE Aqr as per the detection threshold of Fermi-LAT. Van Heerden [18] reported upper limit of 3.47 $\times 10^{-7}$ ph cm^{-2}s^{-1} in the energy range 10 - 100 GeV using pass 7 data and Jian [21] reported upper limit of 1.3 $\times 10^{-12}$ erg cm^{-2}s^{-1} in the 0.1 - 300 GeV using pass 8 data. These results are consistent with our upper limit results not included in this paper. The significance of the source is negligible over the entire energy range. We, therefore, investigated energy bins that contribute more to the possible emission. Our aim was to check if there is any energy bin with significance values above the Fermi detection threshold. In our results, we saw that in most of the energy bins the source is insignificant except for a few energy bins with significance that barely exceed 2σ. The energy range with 2σ significance is above the energy range that is most affected by the background contamination, therefore if this is a false detection it cannot be attributed to the influence of the background.

The TS and residual maps produced for the full energy range did not confirm any significant increase in gamma-ray emission at the target region as compared to the background (see Figure

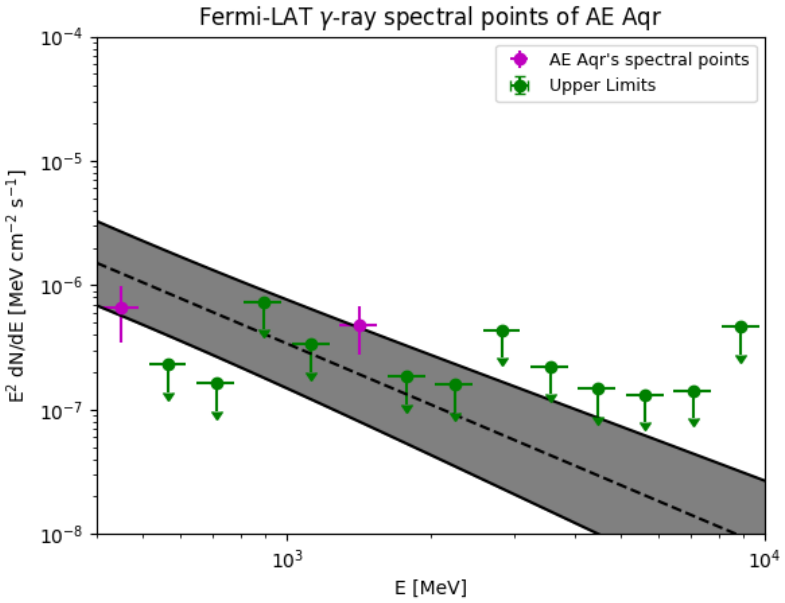

Figure 4: Spectral data points generated on the energy range 0.4-10 GeV, this is the energy range that has the largest significance.

2). The TS map shows that the significance of the target region was less than 2σ significance. This could be because the source is faint due to its proximity to the galactic plane (b = -0.87), which causes an increase in the background. Along the latitude of AE Aqr on the left and right of Figure 2, there are two gamma ray sources that are not modelled because they are not in the 3FGL catalog. Since these sources were not modelled they can influence our results. However, the detection of SED points above the *fermipy* threshold shows that there is a possibility of an increase in gamma-ray activity at the region of AE Aqr. Whether this increased activity is just transient or also periodic in nature and could be linked directly to AE Aqr is still to be investigated further.

Most of the gamma ray Fermi-LAT sources in the ROI are hidden in the background. The background in this region is brighter than most sources as seen in the counts map (see, Figure 1). Even the model map shows that the number of predicted counts for each source still results in some sources with negligible counts (see Figure 1). Therefore the new model of the isotropic diffuse background and the diffuse galactic emission model for the 4FGL catalog will likely produce better results.

Acknowledgements

The authors thank the organisers for the opportunity to present this work at the SAIP 2018 conference. They also want to extend their gratitude to the University of the Free State (UFS) postgraduate school and the UFS Department of Physics for assistance. The financial assistance of the National Research Foundation (NRF) towards this research is also acknowledged. Opinions expressed and conclusions arrived at, are those of the author and are not necessarily to be attributed to the NRF.

References

[1] Joy A H 1954 ApJ **120** 377

[2] Crawford J A and Kraft R P 1956 ApJ **123** 44
[3] Chincarini G and Walker M F 1981 A&A **104** 24–32
[4] Meintjes P J, Odendaal A and van Heerden H J 2015 *Acta Polytechnica CTU Proceedings* **2** 86–89
[5] Zinner E 1938 *Astronomische Nachrichten* **265** 345–352
[6] Wynn G A, King A R and Horne K 1997 MNRAS **286** 436–446
[7] Meintjes P J and Venter L A 2005 MNRAS **360** 573–582
[8] Bookbinder J A and Lamb D Q 1987 ApJ **323** L131–L135
[9] Bastian T S, Dulk G A and Chanmugam G 1988 ApJ **324** 431–440
[10] Patterson J 1979 ApJ **234** 978–992
[11] Eracleous M and Horne K 1996 ApJ **471** 427
[12] Oruru B and Meintjes P J 2012 MNRAS **421** 1557–1568
[13] Venter L A and Meintjes P J 2006 MNRAS **366** 557–565
[14] Meintjes P J 1989 *M.Sc Thesis (Pothefstroom Univ. for CHE)*
[15] Meintjes P J 1992 *Thesis (Potchefstroom Univ. for CHE*
[16] Meintjes P J, De Jager O C, Raubenheimer B C, Nel H I, North A R, Buckley D A H and Koen C 1994 ApJ **434** 292–305
[17] Bowden C C G, Bradbury S M, Chadwick P M, Dickinson J E, Dipper N A, Edwards P J, Lincoln E W, McComb T J L, Orford K J, Rayner S M *et al.* 1992 *ASTROPART PHYS* **1** 47–59
[18] van Heerden H J and Meintjes P J 2015 *Mem. Soc. Astron. Ital.* **86** 111
[19] Acero F, Ackermann M, Ajello M, Albert A, Baldini L, Ballet J, Barbiellini G, Bastieri D, Bellazzini R, Bissaldi E *et al.* 2016 ApJ **223** 26
[20] Mattox J R, Bertsch D, Chiang J, Dingus B, Digel S, Esposito J, Fierro J, Hartman R, Hunter S, Kanbach G *et al.* 1996 ApJ **461** 396
[21] Li J, Torres D F, Rea N, de Ona Wilhelmi E, Papitto A, Hou X and Mauche C W 2016 ApJ **832** 35